

Imaging port wine stains by fiber optical coherence tomography

Shiyong Zhao*

Beijing Institute of Technology
Department of Optoelectronics
Beijing 100081 China

Ying Gu*[†]

Beijing Institute of Technology
Department of Optoelectronics
Beijing 100081 China
and
Chinese PLA General Hospital
Department of Laser Medicine
Beijing 100853 China

Ping Xue

Tsing-Hua University
Department of Physics
Beijing 100081 China

Jin Guo

Fudan University
Department of Chemistry
Shanghai 200433 China
and
Fudan University
Institutes of Biomedical Sciences
Shanghai 200032 China

Tingmei Shen

Beijing Institute of Technology
Department of Optoelectronics
Beijing 100081 China
and
Chinese PLA General Hospital
Department of Laser Medicine
Beijing 100853, China

Tianshi Wang

Tsing-Hua University
Department of Physics
Beijing 100081 China

Naiyan Huang

Chinese PLA General Hospital
Department of Laser Medicine
Beijing 100853 China

Li Zhang

Fudan University
School of Life Sciences
Shanghai 200433 China
and
Fudan University
Institutes of Biomedical Sciences
Shanghai 200032 China

Haixia Qiu

Chinese PLA General Hospital
Department of Laser Medicine
Beijing 100853 China

Xin Yu

Beijing Institute of Technology
Department of Optoelectronics
Beijing 100081 China

Xunbin Wei[†]

Fudan University
School of Life Sciences
Shanghai 200433 China
and
Fudan University
Institutes of Biomedical Sciences
Shanghai 200032 China

Abstract. We develop a fiber optical coherence tomography (OCT) system in the clinical utility of imaging port wine stains (PWS). We use our OCT system on 41 patients with PWS to document the difference between PWS skin and contralateral normal skin. The system, which operates at 4 frames/s with axial and transverse resolutions of 10 and 9 μm , respectively, in the skin tissue, can clearly distinguish the dilated dermal blood vessels from normal tissue. We present OCT images of patients with PWS and normal human skin. We obtain the structural parameters, including epidermal thickness and diameter and depth of dilated blood vessels. We demonstrate that OCT may be a useful tool for the noninvasive imaging of PWS. It may help determine the photosensitizer dose and laser parameters in photodynamic therapy for treating port wine stains. © 2010 Society of Photo-Optical Instrumentation Engineers. [DOI: 10.1117/1.3445712]

Keywords: optical coherence tomography; port wine stains; photodynamic therapy.

Paper 09460R received Oct. 12, 2009; revised manuscript received Apr. 18, 2010; accepted for publication Apr. 20, 2010; published online Jun. 15, 2010.

1 Introduction

Port wine stain (PWS) is a congenital disease with 3 to 5% incidence.^{1,2} The histopathological manifestation is the capillary dilation and malformation in the upper dermis (papillary

*Contributed equally to this work.

[†]Address all correspondence to: Ying Gu, Department of Optoelectronics, Beijing Institute of Technology, and Department of Laser Medicine, Chinese PLA General Hospital, Beijing 100853, China. Tel: 86-10 6693939; Fax: 86-10 68212522; E-mail: guyinglaser@sina.com and Xunbin Wei, School of Life Science, Fudan University, and Institutes of Biomedical Science, Fudan University, Shanghai 200032, China. Tel: 86-21 54237100; Fax: 86-21 54237100; E-mail: xwei@fudan.edu.cn

layer). Photodynamic therapy (PDT), which has been used to treat PWS for the last 2 decade, has advantages including excellent tissue selection, strong lesion effects on microvessels, and few side effects. Therefore, it has become³⁻¹⁰ one of the most effective therapies for PWS. The mechanism of PDT is that, when the endogenous or exogenous photosensitizer in the tissue is exposed to light of a specific wavelength, it absorbs the photon energy and transits to the excited state, then it soon releases energy and relaxes to its ground singlet state through a physical or chemical deexcitation process, during which a large quantity of reactive oxygen is generated. The singlet oxygen reacts with various biomolecules, resulting in cell killing through apoptosis and/or necrosis, as well as an occlusion effect on blood vessels. The key of applying PDT to PWS is to selectively destroy dilated and malformed capillaries in the upper dermis, while sparing the epidermis and deep dermis. PDT has been used for cancer treatment. Khan et al.,¹¹ Wilson et al.,¹² Dougherty et al.,^{13,14} Henderson and Dougherty,¹⁵ and Dougherty^{16,17} used HpD as a photosensitizer combined with red light illumination and achieved good results in treating a dozen of cancer types including breast cancer, uterine cancer, basal cell cancer, and squamous cell carcinoma. The clinical applications become broader as the research on PDT goes deeper. Gu et al. applied PDT in clinical treatment of PWS in 1991 with good clinical effects.¹⁸

Despite the fact that the effects of PDT on PWS microvessels have been widely reported, the area of vessel lesions and the relationship between treatment and efficacy are not clear due to the complex relationship among light, photosensitizer, oxygen, and tissue structure during PDT. The treatment effects in the tissue vary dynamically during the PDT process, and thus are difficult to evaluate in real time accurately. Therefore, the key issue to improve PDT therapeutical efficacy is to have an objective diagnosis and determine the proper drug and laser dosage for an individual patient. Since PWS usually occurs on the face, it is not realistic to conduct common histological observation before and after treatment. Novel noninvasive imaging methods have long being explored. The emergence of optical coherence tomography (OCT), with its main characteristics of *in situ*, *in vivo*, and in real-time use has made the noninvasive detection of skin disease possible. OCT currently has broad applications in highly scattering tissues such as the skin, blood vessels, the urinary bladder, and the splanchnic organs, as well as successful ocular applications.¹⁹⁻²³

Doppler OCT (DOCT), spectroscopic OCT (SOCT), and polarization-sensitive OCT (PS-OCT) have potentially powerful applications in assessing the efficacy of PDT treatment. Blood flow in PWS was measured with DOCT by Zhao et al.²¹ Blood oxygen saturation is an important parameter in PDT. It was measured²² by SOCT according to the absorption coefficient of hemoglobin (Hb) and oxyhemoglobin (HbO₂) at 800 nm. In addition, the depth of skin tissue lesion can be measured by PS-OCT due to birefringence of collagen in dermis.²³ Here, we apply OCT to PWS clinical detection, and obtain the images of epidermis thickness and the configuration of dilated capillary vessels. Doing this will improve the pathological diagnosis and potentially can be used to monitor PDT treatment efficacy in real time.

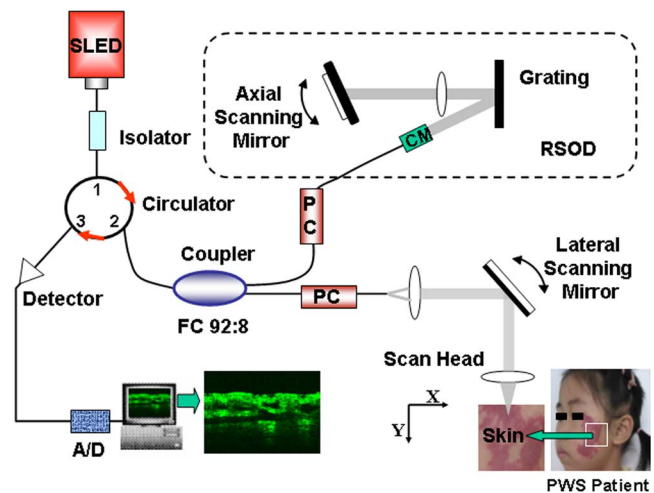


Fig. 1 Schematic of the OCT system.

2 Materials and Methods

Dilated papillaries in the PWS patient dermis is usually within 1 mm below the skin surface with an average diameter over 50 μm , in contrast to a 10- μm diameter in normal skin vessel.^{2,24-28} Therefore, we designed our OCT system with 10- μm axial resolution in skin tissue, determined by light source spectral width.

OCT uses a low-coherence IR light source to detect reflection and scattering echoes from the specimen and builds images of the inner structure. Currently the time domain OCT technique is widely used. We designed and developed a portable time domain OCT system for clinical PWS detection.

Figure 1 shows a schematic of our OCT imaging system. It employs a superluminescent LED (SLED) broadband light source with a central wavelength at 1310 nm and a spectral FWHM of 70 nm. To eliminate the system reflection on the light source, the source output is first connected to an optical isolator via a pigtail fiber, and then coupled to a 92:8 fiber coupler by a three-port optical circulator. The coupler passes 92% of the light to the sample arm and 8% to the reference arm. Light reflected from the sample arm and the reference arm interferes at the coupler. It is further converted into the current signal by *a-p-i-n* photodiode and preamplified by a current amplifier, which converts the weak current signal into a voltage signal. Before being sent to a data acquisition card, the output signal is amplified by a low-noise preamplifier and filtered by a bandpass filter. A 12-bit analog-to-digital (A/D) converter samples and quantifies the output analog signal. Then digital bandpass filter further removes the noise. After digital signal processing (DSP), structure OCT image is generated based on the amplitude of axial scanning. The sample arm and the reference arm are equipped with polarization controllers (PC1 and PC2) to control the polarization mode of light output.

The reference arm employs the grating rapid scanning optical delay (RSOD) line, shown by the dashed-line part in Fig. 1, which realizes axial scanning with a resonant scanning frequency²⁹ at 800 Hz, carrier wave central frequency at 1163 kHz, and a 383-kHz bandwidth. The delay line is used for the carrier wave central frequency setup and dispersion

Table 1 Parameters of epidermis and dilated blood vessels determined by OCT images ($n=41$, data presented as mean±standard deviation).

	PWS Skin (μm)	Contralateral Normal Skin (μm)
Epidermal thickness	64.61 ± 16.60	64.83 ± 17.01
Diameter of blood vessels	94.61 ± 20.09	rarely seen
Depth of blood Vessel	360.70 ± 50.20	rarely seen

Note: The used mean skin index of refraction³²⁻³⁴ at 1310 nm is 1.36.

compensation, shown by the dashed frame. The grating and the swaying mirror are placed on the front and back focus planes, respectively, which can optimize dispersion match.^{30,31}

The sample arm is equipped with a handheld detector that scans laterally. It consists of a fiber collimator, a scanning mirror and an achromatic lens. The spot size of the beam focused on the specimen determines the lateral resolution of the OCT system. The numerical aperture of the objective determines the speckle size. The detector consists of a swaying mirror and an achromatic lens. The rotation of the swaying mirror produces lateral scanning at various positions. A lens with a focal length of 20 mm is chosen, via which the beam is focused onto the sample with a focus 9- μm -diam which is the lateral resolution of the OCT system. This matches the axial resolution, and therefore avoids image distortion.

In addition, all fiber ends in the system are coated with antireflection film to greatly improve the SNR. The measured SNR of the OCT system is 108 dB.

3 Results and Discussion

The human skin is composed of epidermis and dermis. The thickness range of the epidermis is from 0.04 to 1.6 mm, and about 0.1 mm on average.^{27,28} It varies greatly among individuals. The dermis is beneath the epidermis and is generally divided into two layers: the papillary layer and the reticular

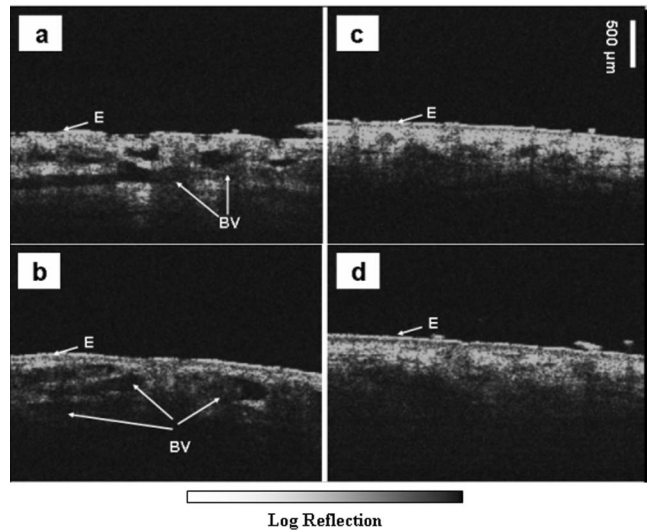


Fig. 3 OCT images of right lower eyelid, right upper lip, and their contralateral normal skin of patient 1.

layer. The consideration of PDT for PWS treatment focuses on the thickness of the epidermis and the vascular distribution in the dermis papillary layer.

Forty-one Chinese patients with PWS on the face and neck (18 males and 23 females, aged from 0.9 to 45 years, 8.81 ± 8.72 years old) were recruited from among the outpatients of the Department of Laser Medicine, Chinese PLA General Hospital. This study was approved by Ethics Committee of the Chinese PLA General Hospital. OCT images of PWS skin and their contralateral normal skin were acquired from multiple sites of the 41 patients. The structural parameters, including epidermal thickness and diameter and depth of dilated blood vessels, were obtained. The average and spread of the key parameters are displayed in Table 1. Photos and OCT images of five typical patients are displayed in Figs. 2–11 as follows. Figures 2, 4, 6, 8, and 10 show PWS areas and contralateral normal face skin, scanned by the OCT system. The scanning area is 1.8 mm (lateral) by 2.5 mm (axial)

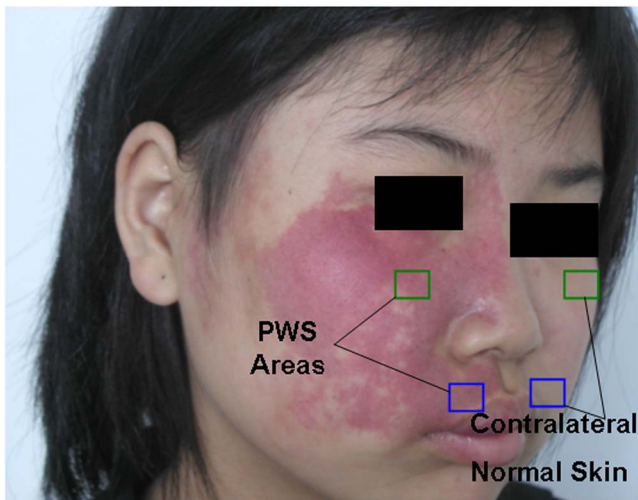


Fig. 2 Areas scanned by the OCT system of patient 1.

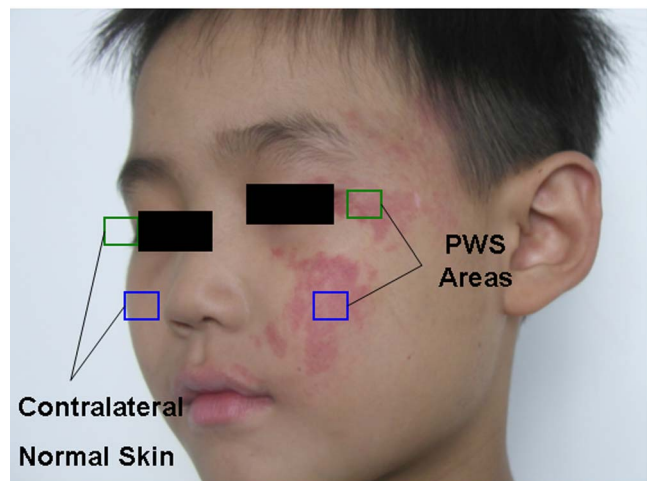


Fig. 4 Areas scanned by the OCT system of patient 2.

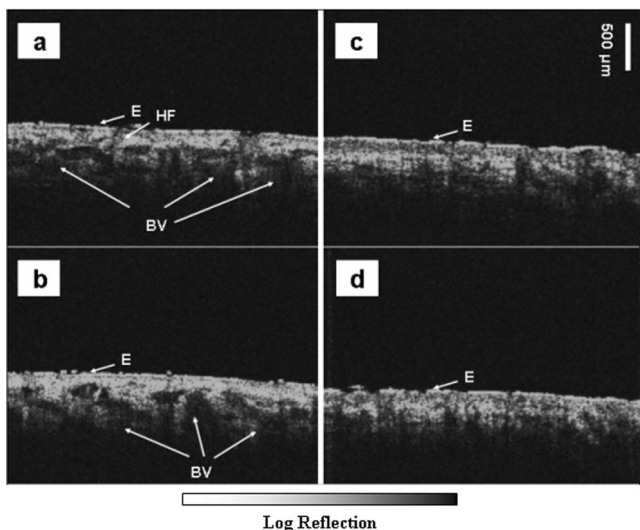


Fig. 5 OCT images of left outer canthus, left pars zygomaticus, and the contralateral normal skin of patient 2.

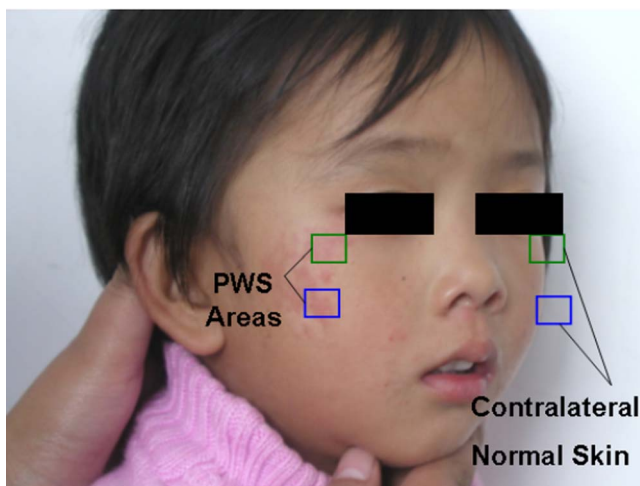


Fig. 6 Areas scanned by the OCT system of patient 3.

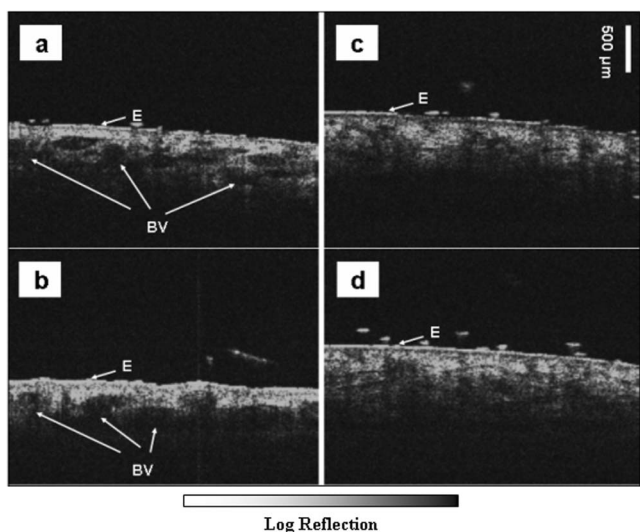


Fig. 7 OCT images of right pars zygomaticus, right buccal division, and the opposite normal skin of patient 3.

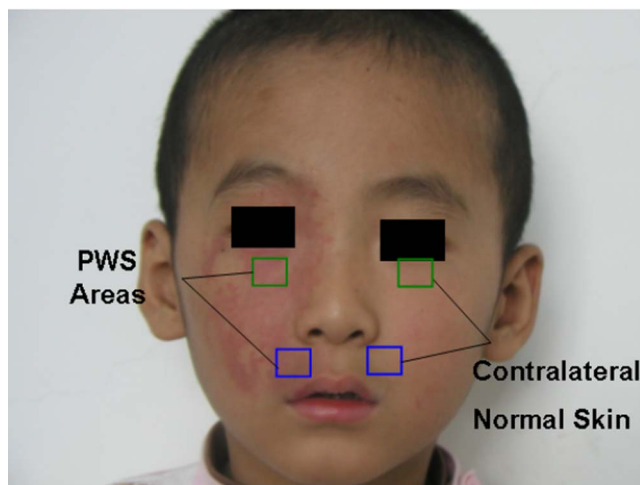


Fig. 8 Areas scanned by the OCT system of patient 4.

with a scanning speed of 4 frames/s. Corresponding gray-scale OCT images (Figs. 3, 5, 7, 9, and 11, where E indicates the epidermis and BV represents blood vessels) show different structures between PWS areas and contralateral normal skin. We are able to distinguish the dilated capillary vessels from normal tissue, based on blood vessel diameter and configuration. There are many “black holes” with “shadow effect” from pathological skin, in contrast to the contralateral normal skin. Normally large diameter blood vessels would produce a “shadow effect” in the B-scan OCT images because the blood has slightly more absorption of light and results in the image loss beyond the point of the proximal vessel.³⁵⁻³⁸ From these OCT images, we obtained the similar results that “black holes” are displayed in PWS areas and rarely found in contralateral normal skin. As the average diameter of contralateral vessels in normal skin is²⁶ about 10 μm , the vascular structure of normal skin cannot be displayed clearly with the resolution of our current OCT system. However, the di-

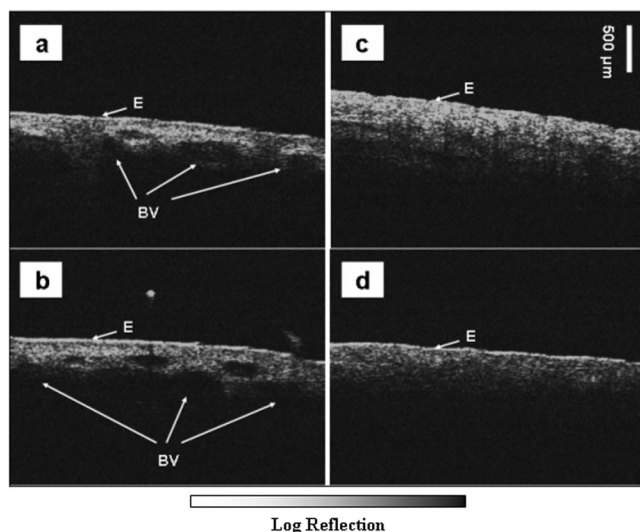


Fig. 9 OCT images of right lower eyelid, right upper lip, and the contralateral normal skin of patient 4.

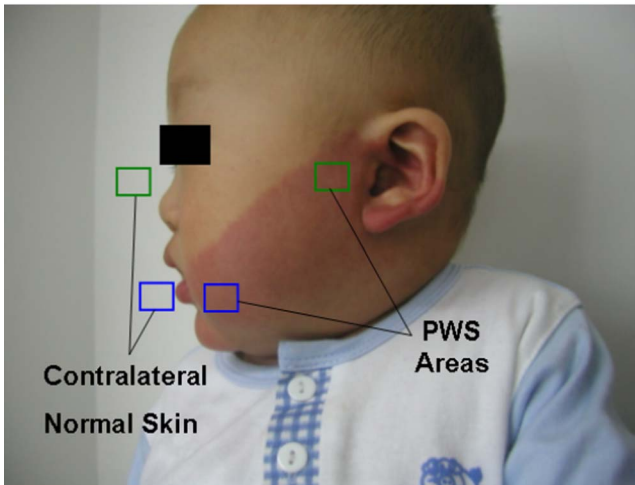


Fig. 10 Areas scanned by the OCT system of patient 5.

ameter of dilated capillary vessels in patients with PWS are usually²⁶ larger than $50\ \mu\text{m}$. Therefore, the dilated capillary network in the papillary layer in PWS patients can be distinguished.

The measured mean diameter and depth of the vessels from 41 PWS patients in our study are $94.61 \pm 20.09\ \mu\text{m}$ and $360.70 \pm 50.20\ \mu\text{m}$, respectively. The mean blood vessels diameter fit well with the typical biopsy and confocal microscopy study²⁶ ($87.72 \pm 3.21\ \mu\text{m}$). The mean blood vessels depth from OCT images correlates (although it is somewhat smaller) with those results obtained by the biopsy (Barsky et al.² and Zhou et al.²⁴ obtained the mean vessel depths of 0.46 ± 0.1 and 0.45 ± 0.2 mm, respectively). The difference might be due to the OCT penetration limit where some blood vessels could not be detected in deeper tissue. Furthermore, thickness of epidermis was obtained in Table 1. The measured mean epidermal depth of PWS skin and contralateral normal skin are 64.61 ± 16.60 and $64.83 \pm 17.01\ \mu\text{m}$, respectively. There is no statistical difference between them.

PDT for PWS requires the simultaneous presence of a laser, a photosensitizer, and singlet oxygen. Therapeutic efficacy depends on laser dosage, photosensitizer concentration, and tissue oxygenation level. Optimal treatment outcome can be achieved only when these three parameters are closely matched. Epidermal thickness correlates with laser dosage, due to the epidermal absorption and scattering of light. For example, adults are given $100\ \text{mW}/\text{cm}^2$ laser treatment in PDT, while $60\ \text{mW}/\text{cm}^2$ laser intensity is given to children, since the adults epidermis is thicker than that of children.^{39,40}

The diameter of blood vessels relates with the oxygenation levels in PDT. In our previous mathematical model study,⁴¹ lower oxygenation levels distribute in large-diameter blood vessels than that in small blood vessels. This is why PDT for light-red-color PWS patients usually achieves a better therapeutic effect than that for dark-red-color ones. In addition, clinicians observe that the first PDT therapy often achieves good results, although the therapeutic effect decreases with the number of therapies in the same PWS patient. We speculate that the shallow blood vessels have been first removed, therefore the same laser dosage is not enough to remove deep

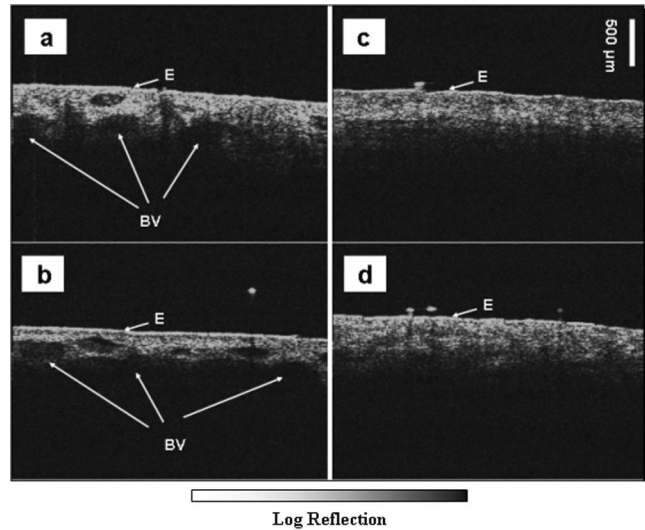


Fig. 11 OCT images of left anterior auricular, left corner of the mouth, and the contralateral normal skin of patient 5.

blood vessels. The depth of blood vessels from OCT images will be helpful to study the relationship between therapeutic effect and therapeutic times.

In the past, when applying PDT to PWS treatment, doctors chose drug dose and laser parameters (wavelength, exposure duration, laser power intensity) mainly according to the color of the red stain (the color of PWS areas mainly due to dilation degree of capillary vessels in papillary layer) and skin hyperplasia. It is difficult to diagnose pathological types because the thickness of skin varies from patient to patient and the thickness distribution of skin in different part of the same patient also varies. There are certain errors to adopting a similar treatment to different pathological types. Furthermore, diagnosis of pathological types is influenced by pigments in patient skin and by visual judgment of doctors. We are currently investigating 3-D OCT and Doppler OCT, which will provide further details on the configuration and blood flow of the capillary vessels, epidermis structures, papillary layers, and dermis. Doctors can make objective judgments of pathological types according to the thickness of the epidermis and the diameter and depth of dilated blood vessels. In conclusion, the anatomical parameters provided by OCT are very meaningful for both clinical treatment dosage and the judgment of treatment effects.

4 Conclusions

We implemented an OCT system capable of distinguishing the dilated capillary vessels from normal tissue and the thicknesses of the epidermis and the papillary layer. The imaging rate of the OCT system is 4 frames/s with axial and transverse resolution being 10 and $9\ \mu\text{m}$, respectively in the skin tissue. The imaging results demonstrated that OCT is a promising tool of noninvasive “optical sectioning” for clinical PWS treatment.

Acknowledgments

This work is partially supported by the National Basic Research Program of China (Grant No. 001CB510307), the Hi-

tech Research and Development Program of China (Grant No. 2006AA02Z472), the China National Key Projects for Infectious Disease (Grant No. 2008ZX10002-021), the National Natural Science Foundation of China (Grants 60878055, 90508001, 10574081, and 30770524), the Natural Science Foundation of Beijing (Grant No. 3072012), and the Excellent Talent Supporting Project in the New Century of the Chinese Education Ministry (Grant No. NCET-08-0131).

References

1. A. H. Jacobs and R. G. Walton, "The incidence of birthmarks in the neonate," *Pediatrics* **58**, 218–222 (1976).
2. S. H. Barsky, S. Rosen, D. E. Geer, and J. M. Noe, "The nature and evolution of port-wine stains: a computer-assisted study," *J. Invest. Dermatol.* **74**, 154–157 (1980).
3. T. K. Smith, B. Choi, J. C. Ramirez-San-Juan, J. S. Nelson, K. Osann, and K. M. Kelly, "Microvascular blood flow dynamics associated with photodynamic therapy, pulsed dye laser irradiation and combined regimens," *Lasers Surg. Med.* **38**, 532–539 (2006).
4. L. O. Svaasand, G. Aguilar, J. A. Viator, J. S. Nelson, et al., "Increase of dermal blood volume fraction reduces the threshold for laser-induced purpura: implications for port wine stain laser treatment," *Lasers Surg. Med.* **34**, 182–188 (2004).
5. D. W. Edstrom, M. A. Hedblad, and A. M. Ros, "Flashlamp pulsed dye laser and argon-pumped dye laser in the treatment of port wine stains: a clinical and histological comparison," *Br. J. Dermatol.* **146**, 285–289 (2002).
6. P. Babilas, G. Shafirstein, W. Baumler, J. Baier, M. Landthaler, R. M. Szeimies, and C. Abels, "Selective photothermolysis of blood vessels following flashlamp-pumped pulsed dye laser irradiation: *in vivo* results and mathematical modeling are in agreement," *J. Invest. Dermatol.* **125**, 343–352 (2005).
7. L. T. Norvang, E. J. Fiskerstrand, J. S. Nelson, M. W. Berns, and L. O. Svaasand, "Epidermal melanin absorption in human skin," *Proc. SPIE* **2624**, 143–154 (1996).
8. Y. Wang, Y. Gu, X. Liao, R. Chen, and H. Ding, "Fluorescence monitoring of a photosensitizer and prediction of the therapeutic effect of photodynamic therapy for port wine stains," *Exp. Biol. Med.* **235**, 175–180 (2010).
9. M. J. Van Gemert, D. J. Smithies, W. Verkruyse, T. E. Milner, and J. S. Nelson, "Wavelengths for port wine stain laser treatment: Influence of vessel radius and skin anatomy," *Phys. Med. Biol.* **42**, 41–50 (1997).
10. M. Sickenberg et al., "A preliminary study of photodynamic therapy using verteporfin for choroidal neovascularization in pathologic myopia, ocular histoplasmosis syndrome, angioid streaks, and idiopathic causes," *Arch. Ophthalmol.* **118**, 327–336 (2000).
11. S. A. Khan, T. J. Dougherty, and T. S. Mang, "An evaluation of photodynamic therapy in the management of cutaneous metastases of breast cancer," *Eur. J. Cancer* **29**(12), 1686–1690 (1993).
12. B. D. Wilson, T. S. Mang, H. Stoll, C. Jones, M. Cooper, and T. J. Dougherty, "Photodynamic therapy for the treatment of basal cell carcinoma," *Arch. Dermatol.* **128**(12), 1597–1601 (1992).
13. T. J. Dougherty, J. E. Kaufman, A. Goldfarb, K. R. Weishaupt, D. Boyle, and A. Mittleman, "Photoradiation therapy for the treatment of malignant tumors," *Cancer Res.* **38**, 2628–2635 (1978).
14. T. J. Dougherty, C. J. Gomer, B. W. Henderson, G. Jori, D. Kessel, M. Korbelik, J. Moan, and Q. Peng, "Photodynamic therapy," *J. Natl. Cancer Inst.* **90**, 889–905 (1998).
15. B. W. Henderson and T. J. Dougherty, "How does photodynamic therapy work?" *Photochem. Photobiol.* **55**, 145–157 (1992).
16. T. J. Dougherty, "Photoradiation therapy for cutaneous and subcutaneous malignancies," *J. Invest. Dermatol.* **77**(1), 122–124 (1981).
17. T. J. Dougherty, "An update on photodynamic therapy applications," *J. Clin. Laser Med. Surg.* **20**, 3–7 (2002).
18. Y. Gu, J. Li, Y. Jiang, J. Liang, P. Zhou, X. Cui, Y. Pan, and K. Wang, "A clinical study of photodynamic therapy for port wine stains—a report of 40 cases," *Chin. J. Laser Med. Surg.* **1**(1), 6–10 (1992).
19. J. M. Schmitt, "Optical coherence tomography (OCT): a review," *IEEE J. Sel. Top. Quantum Electron.* **5**(4), 1205–1215 (1999).
20. Y. Pan, J. Lavelle, S. Bastaky, D. Farkas, and M. Zeidel, "Noninvasive imaging and analysis of biological tissue structure, function and abnormalities with optical coherence tomography," *Proc. SPIE* **4224**, 391–399 (2003).
21. Y. Zhao, Z. Chen, C. Saxer, Q. Shen, S. Xiang, J. F. de Boer, and J. S. Nelson, "Doppler standard deviation imaging for clinical monitoring of *in vivo* human skin blood flow," *Opt. Lett.* **25**(18), 1358–1360 (2000).
22. L. E. Kagemann, G. Wollstein, M. Wojtkowski, et al., "Spectral oximetry assessed with high-speed ultra-high-resolution optical coherence tomography," *J. Biomed. Opt.* **12**(4), 041212 (2007).
23. B. E. Applegate, C. Yang, A. M. Rollins, and J. A. Izatt, "Polarization-resolved second-harmonic-generation optical coherence tomography in collagen," *Opt. Lett.* **29**(19), 2252–2254 (2004).
24. G. Zhou, Z. Zhang, et al., "Computed assessment of pathological images on 52 case biopsies of port wine stain," *Chin. J. Oral Maxillofac Surg.* **9**(2), 112–115 (1999).
25. G. Argenziano, I. Zalaudek, R. Corona, F. Sera, L. Cicale, G. Petrillo, E. Ruocco, R. Hofmann-Wellenhof, and H. P. Soyer, "Vascular patterns in skin tumors, a dermoscopy study," *Arch. Dermatol.* **140**(12), 1485–1489 (2004).
26. C. Chang, J. Yu, and J. S. Nelson, "Confocal microscopy study of neurovascular distribution in facial port wine stains (capillary malformation)," *J. Formos Med. Assoc.* **107**(7), 559–566 (2008).
27. R. R. Anderson and J. A. Parrish, "The optics of human skin," *J. Invest. Dermatol.* **77**, 13–19 (1981).
28. I. V. Meglinsky and S. J. Matcher, "Modelling the sampling volume for skin blood oxygenation measurements," *Med. Biol. Eng. Comput.* **39**(1), 44–50 (2001).
29. A. M. Rollins, M. D. Kulkarni, S. Yazdanfar, R. Ung-arunyawee, and J. A. Izatt, et al., "*In vivo* video rate optical coherence tomography," *Opt. Express* **3**, 219–229 (1998).
30. G. J. Tearney, B. E. Bouma, and J. G. Fujimoto, "High-speed phase-and group-delay scanning with a grating-based phase control delay line," *Opt. Lett.* **22**, 1811–1813 (1997).
31. W. K. Niblack, J. O. Schenk, B. Liu, and Mark E. Brezinski, "Dispersion in a grating-based optical delay line for optical coherence tomography," *Appl. Opt.* **42**, 4115–4118 (2003).
32. G. J. Tearney, M. E. Brezinski, J. F. Southern, B. E. Bouma, M. R. Hee, and J. G. Fujimoto, "Determination of the refractive index of highly scattering human tissue by optical coherence tomography," *Opt. Lett.* **20**, 2258–2260 (1995).
33. A. Knüttel and M. Boehlau-Godau, "Spatially confined and temporally resolved refractive index and scattering evaluation in human skin performed with optical coherence tomography," *J. Biomed. Opt.* **5**, 83–92 (2000).
34. H. Ding, J. Lu, W. A. Wooden, P. J. Kragel, and X. Hu, "Refractive indices of human skin tissues at eight wavelengths and estimated dispersion relations between 300 and 1600 nm," *Phys. Med. Biol.* **51**, 1479–1489 (2006).
35. J. K. Barton, A. J. Welch, and J. A. Izatt, "Investigating pulsed dye laser-blood vessel interaction with color Doppler optical coherence tomography," *Opt. Express* **3**(6), 251–256 (1998).
36. J. K. Barton, A. Rollins, J. A. Izatt, et al., "Photothermal coagulation of blood vessels: a comparison of high-speed optical coherence tomography and numerical modeling," *Phys. Med. Biol.* **46**, 1665–1678 (2001).
37. M. H. Khan, B. Choi, S. Chess, K. M. Kelly, J. McCullough, and J. S. Nelson, "Optical clearing of *in vivo* human skin: implications for light-based diagnostic imaging and therapeutics," *Lasers Surg. Med.* **34**, 83–85 (2004).
38. J. M. Ridgway, W. B. Armstrong, S. Guo, U. Mahmood, J. Su, R. P. Jackson, T. Shibuya, R. L. Crumley, M. Gu, Z. Chen, and B. J. Wong, "*In vivo* optical coherence tomography of the human oral cavity and oropharynx," *Arch. Otolaryngol. Head Neck Surg.* **132**, 1074–1081 (2006).
39. Y. Gu, N. Huang, F. Liu, J. Liang, and Y. Pan, "Clinical study of 1949 cases of port wine stains treated with vascular photodynamic therapy," *Ann. Dermatol. Venereol.* **134**, 241–244 (2007).
40. N. Huang, "What is the optimal PDT protocol for treating port wine stains (PWS)?" *Photodiagn. Photodyn. Therapy* **4**, 145–146 (2007).
41. N. Huang, Y. Gu, F. Liu, G. Cheng, Q. Zhong, Y. Wang, and G. Zhao, "Preliminary exploration of mathematical simulation of photodynamic treatment on port wine stains' reaction system," *Chin. J. Laser Med. Surg.* **14**, 83–89 (2005).